Langmuir

ARTICLE

pubs.acs.org/Langmuir

Amphiphile Disruption of Pathogen Attachment at the Hematite (α-Fe_2O_3)−Water Interface

Xiaodong Gao and Jon Chorover*

Department of Soil, Water and Environmental Science, University of Arizona, Tucson, Arizona 85721, United States

Supporting Information

ABSTRACT: Prior studies have indicated that the subsurface transport of *Cryptosporidium parvum* oocysts is diminished in sediments containing iron oxides and that inner-sphere complexation of oocyst surficial carboxylate plays a role in the retardation. However, the impacts of natural organic matter (NOM) remain poorly understood. In this study, we used a model anionic surfactant, sodium dodecyl sulfate (SDS), as a surrogate for amphiphilic NOM components to examine the impacts of amphiphilic components on oocyst adhesion mechanisms. We employed in situ attenuated total reflectance Fourier transform infrared (ATR-FTIR) spectroscopy to determine the effects of SDS on the molecular bonds that mediate interactions between oocyst surficial biomolecules and hematite (α-Fe_2O_3) surface functional groups over a wide range of solution pH. The results show that the presence of SDS significantly diminishes Fe−carboxylate complexation, as indicated by progressive decreases in intensity of asymmetric and symmetric stretching vibrations of carboxylate [$\nu_{as}(COO^-)$ and $\nu_s(COO^-)$] with reaction time. In addition, one of the $\nu_s(COO^-)$ bands shifted from 1370 to 1418 cm^{-1} upon SDS introduction, suggesting that SDS also changed the complexation mode. The data indicate that competition from the sulfonate groups (OSO_3^-) of SDS at α-Fe_2O_3 surface sites is a primary mechanism resulting in decreased Fe−carboxylate complexation. Sorptive competition from amphiphilic NOM components may therefore increase the mobility of *C. parvum* oocysts in the environment through disruption of interfacial pathogen−mineral surface bonds.

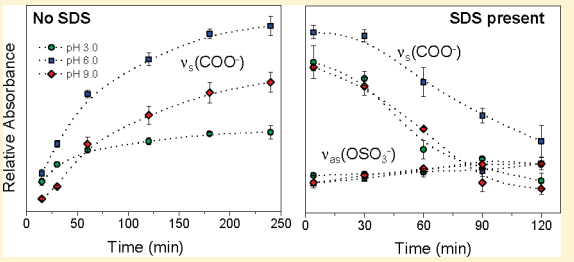

1. INTRODUCTION

Microbial cells, such as bacteria and protozoa, can be transported over relatively long distances in porous geomedia prior to adhering to mineral or organic surfaces because, like much of the geomedia itself, microbial surfaces usually carry a net negative charge.[1,2] Adhesion of microbial cells to substrate surfaces is primarily governed by microbe−mineral interfacial forces.[3] Prior experiments indicate that long-range electrostatic forces and short-range steric forces both play important roles in cell transport and adhesion to surfaces.[3−5] For example, coating of negative-charged quartz sand with positive-charged iron oxides increases microbial cell adhesion.[6,7] In addition, several recent spectroscopic studies have observed direct chemical bonding between surface biomolecular functional groups and hydroxylated mineral surfaces. Inner-sphere complexation of phosphate/phosphonate[8] and carboxylate groups[9] with Fe(III) metal centers was observed during bacterial adhesion to the hematite surface. The formation of H-bonds between bacterial surficial polysaccharides and metal oxide (e.g., goethite, TiO_2, and Al_2O_3) surface hydroxyl groups has also been reported.[10,11]

Cryptosporidium parvum is a water-borne protozoan pathogen that is responsible for the gastrointestinal disease cryptosporidiosis, which is potentially lethal for immunocompromised individuals.[12] Oocysts, the encysted, environmental form of the obligate pathogen, exhibit a complex mixture of surface bio macromolecules, consisting primarily of amide, carboxylate, phosphate, and polysaccharide functionalities.[13,14] Ionizable functional groups, such as carboxylate and phosphate groups, may serve as reactive sites for direct bonding to mineral surfaces. For example, in a previous spectroscopic study, we found that oocysts form either inner-sphere or outer-sphere complexes between the surface carboxylate groups and hematite surface, depending on solution chemistry.[15] Such chemical bonding likely contributes to the observed retardation of oocyst transport in Fe-rich geomedia.[6]

Ionic surfactants are important amphiphilic and surface-active components of organic matter that are ubiquitous in the environment.[16,17] Their admicellar and bilayer formations at mineral surfaces have long been thought to be a central feature of natural organic matter (NOM) adsorption to mineral surfaces,[16] and their aggregation behavior is a model representation of NOM supramolecular structure.[17] As such, ionic surfactants may play an important role in mediating the fate and transport of pathogenic cells in the subsurface. For example, as shown by colloidal electrophoresis, anionic surfactants can change or even reverse the surface charge of metal oxides by forming monolayer or bilayer patches on the surfaces.[18,19] Hence, adsorption of surfactants to iron or aluminum (oxyhydr)oxide surfaces (i.e., prevalent in

Received: December 9, 2010
Revised: March 25, 2011
Published: April 13, 2011

geomedia and otherwise positively charged at circumneutral pH) could diminish oocyst adhesion due to an increase in the electrostatic repulsive force. In addition, surfactant adsorption to oxide surfaces can introduce repulsive steric effects such as that characterized by the negative entropy of surfactant−biopolymer mixing.[20] Conversely, it is possible that, insofar as surfactant adsorption increases sorbent hydrophobicity, oocyst adhesion could be enhanced via hydrophobic interaction. To the extent that ionic surfactant molecules form mineral−surface complexes,[19,21,22] they may compete directly with oocyst surface biomolecules for reactive mineral−surface sites.

Despite the prevalence of natural and anthropogenic surfactants and amphiphiles in waters contaminated with *C. parvum* oocysts, their influence on oocyst fate and transport remains poorly understood. Hence, for the purposes of the study described here, we used a well-defined model of synthetic anionic surfactant, sodium dodecyl sulfate (SDS), because its reactivity at (oxyhydr)oxide mineral surfaces is already relatively well-known.[19,21,23] SDS has also been previously studied in cell transport experiments. In a column transport study, Johnson et al.[24] reported that addition of SDS significantly decreased retention of *Acrossocheilus paradoxus* cells in quartz sand and glass bead minicolumns and thereby enhanced cell transport through the porous media. Similarly, effluent recovery of oocysts from soil columns increased by 10-fold at pH 5.0−6.0 when 0.1 mM SDS was introduced to the influent oocyst suspension.[25] The authors attributed the increase in cell transport to surface charge modification on either the microbial cells or the substrate solid surfaces by the surfactant molecules. Interpretation of the data in these studies did not consider potential steric or chemical interactions (i.e., chemical bond formation) in the cell−SDS−mineral surface ternary systems, although these effects may be significant as well.[3,15,26] In any case, without molecular-scale information, it is not possible to know unambiguously the precise mechanisms whereby SDS affects microbial transport.

Given the molecular heterogeneity of NOM, the relative importance of electrostatic, steric, and hydrophobic effects on cell-surface adhesion is likely to depend on the various types of adsorbed NOM present. Therefore, the objective of the current work was to use SDS as a model to probe the effect of amphiphile-type NOM components on oocyst adhesion to the surface of a model Fe(III) oxide (hematite, α-Fe_2O_3) across a gradient in pH that is representative of natural pore waters present in soils and sediments. We employed in situ attenuated total reflectance-Fourier transform infrared (ATR-FTIR) spectroscopy to measure the effects of SDS on oocyst−hematite bonding in the ternary (SDS-containing) system through direct comparison with experiments conducted on SDS-free oocyst suspensions. By examining dynamic changes in spectral data, molecular interaction mechanisms were determined. The results indicate that the presence of SDS can disrupt inner-sphere carboxylate−Fe(III) complexes that tend to form in its absence, providing a molecular mechanism for enhanced transport of oocysts in porous media containing surfactant molecules such as SDS or naturally occurring biosurfactants.

2. MATERIALS AND METHODS

2.1. Chemicals and Solution Preparation. All chemicals used were reagent grade or better. SDS (99%) was purchased from Sigma-Aldrich Co. (St. Louis, MO) and used as received. All solutions and suspensions were prepared using Barnstead Nanopure (BNP) water. Both batch adsorption and ATR-FTIR spectroscopic experiments were conducted in a 10 mM NaCl background electrolyte solution with HCl or NaOH additions as required to give solution pH from 3.0 to 9.0.

2.2. Oocyst Source and Preparation. Viable *C. parvum* oocysts were obtained from the Sterling Parasitology Laboratory (SPL) at the University of Arizona. The supplier separated the oocysts from a calf infected with the Iowa isolate of *C. parvum* at the National Animal Disease Center in Ames, IA, followed by discontinuous sucrose and cesium chloride gradient centrifugation. The oocysts were stored at 4 °C in an antibiotic solution containing 0.01% Tween 20, 111 U of penicillin, 111 U of streptomycin, and 100 μg mL^{-1} of gentamicin. Öocyst size was determined to be 3.88 μm in diameter by immunofluorescent flow cytometry analysis of DAPI-stained cells (Bio-Rad, HS Bryte).[13] Prior to performing the ATR-FTIR experiments, oocysts were washed and resuspended to give a final cell concentration of 2×10^7 mL^{-1} in 10 mM NaCl background electrolyte.[13] The suspension pH was adjusted to 3.0, 4.5, 6.0, 7.5, and 9.0 using 10 mM HCl or NaOH solutions.

2.3. Hematite Synthesis and Characterization. Colloidal hematite (α-Fe_2O_3) used in this study was prepared from the hydrolysis of $Fe(NO_3)_3 \cdot 9H_2O$ (J.T. Baker) at elevated temperature (100 °C) followed by dialysis at pH 4.0 using the methods of Schwertmann and Cornell.[27] Synchrotron X-ray diffraction (XRD) (Beamline 11-3, Stanford Synchrotron Radiation Lightsource), transmission electron microscopy (TEM) (Philips FEI CM12 STEM), and ζ-potential analysis (Brookhaven Instruments ZetaPLAS) were employed to characterize the synthetic material. The results confirmed the material as pure hematite with particle size ~10−20 nm in diameter and a measured isoelectric point (IEP) ~7.7−7.8 in 1 mM $NaNO_3$ background electrolyte.[15]

2.4. Batch Adsorption Experiments. Adsorption envelope experiments were conducted at room temperature to examine the adsorption of SDS on oocysts as a function of pH in batch mode using acid-washed 1.7 mL microcentrifuge tubes as reaction vessels. Experiments were carried out in 1 mL suspension in 10 mM NaCl background electrolyte containing 0.1 mM SDS (14.4 mg L^{-1} C) and 2×10^7 oocysts (ca. 1 g L^{-1} oocysts). The pH of the suspension was adjusted to desired values (pH 3.0−9.0) using 10 mM HCl or NaOH solutions. All experiments were run in duplicate, and adsorbent-free controls (no oocysts) were reacted concurrently for each pH to monitor SDS loss during the reaction process.

The suspensions were equilibrated on an end-over-end shaker (7 rpm) for 24 h reaction time, after which time the pH was remeasured, and samples were then centrifuged at 17 900*g* for 30 min using an Eppendorf 5417C microcentrifuge with a fixed-angle rotor. The supernatant was aspirated and filtered through a 0.45 μm nominal pore size syringe filter with a hydrophilic polypropylene membrane. The dissolved SDS concentration was determined by measuring the sulfur concentration in solutions acidified to pH <2 with trace metal grade HNO_3 using inductively coupled plasma-optical emission spectrometry (ICP-OES) (Perkin-Elmer Optima 5300 DV). The amount of adsorbed SDS was calculated from the difference between the total concentration and that remaining in the supernatant solution following reaction.

2.5. FTIR Spectroscopy Measurements. ATR-FTIR spectra were obtained on (i) SDS-free oocyst suspensions, (ii) 0.1 mM SDS solution alone, and (iii) oocyst suspensions in the presence of 0.01 mM SDS on a hematite-coated ZnSe internal reflection element (IRE). An SDS concentration of 0.01 mM (equivalent to 1.44 mg L^{-1} C) was used in the ternary system because preliminary ATR-FTIR data indicated that even such low SDS concentrations, well below the critical micelle concentration of ~8.1 mM, still resulted in substantial changes in oocyst adhesion. The hematite-coated ZnSe IRE was prepared by evenly spreading a colloidal hematite suspension (500 μL of stock suspension with a solids concentration of 3.3 g L^{-1}) onto the IRE surface and drying

the coating in a vacuum oven (10 mmHg) overnight at room temperature.[15] The thickness of the hematite coating was calculated to be ca. 0.6 μm. The spectra were collected as a function of pH (3.0−9.0) and time (0−120 min after sample introduction) using a Magna-IR 560 Nicolet spectrometer (Madison, WI) equipped with a CsI beam splitter and a deuterated triglycine sulfate (DTGS) detector. The spectrometer was continuously purged with CO_2-free air to eliminate CO_2 absorption. A volatile liquid cover was used to prevent solvent evaporation during the measurement.

For each solution chemistry condition, a 500 μL aliquot of SDS solution or oocyst suspension was applied directly by pipet to the hematite-coated 45° ZnSe IRE in a trough-style sample holder (56 mm ×10 mm ×3 mm) (PIKE Technologies, Inc.). Appropriate background spectra (e.g., 10 mM NaCl or 0.01 mM SDS in 10 mM NaCl) were collected under the same condition. All spectra were acquired at 4.0 cm^{-1} resolution with 400 scans over the spectral range of 4000−800 cm^{-1} without ATR correction for wavenumber dependence. A final sample spectrum was obtained by subtracting the appropriate background spectrum from the sample spectrum. Data collection and spectral processing, including subtraction and baseline correction, were performed using the program OMNIC (Thermo Nicolet Co.) and the GRAMS/AI spectral software package.

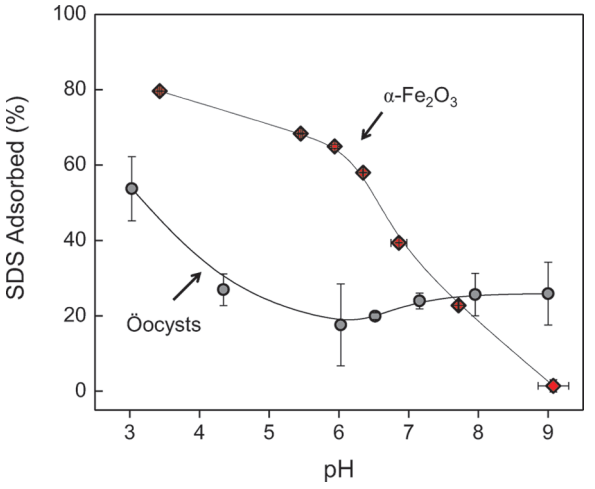

Figure 1. Fraction of SDS adsorbed by oocyst suspension as a function of pH in 10 mM NaCl electrolyte solution after 24 h reaction time (0.1 mM SDS and 1 g L^{-1} oocysts). SDS adsorption envelope on hematite from Gao and Chorover[21] is shown for direct comparison (0.1 mM SDS and 5.0 g L^{-1} hematite).

3. RESULTS AND DISCUSSION

3.1. SDS−Hematite Binary System. ATR-FTIR spectra of SDS on the α-Fe_2O_3 surface exhibit strong pH dependence (Figure S1 in the Supporting Information). The spectra contain two major spectral regions, corresponding to the hydrophobic tail (3000−2800 cm^{-1}) and hydrophilic sulfonate head (1250−950 cm^{-1}), respectively.[19,21,23] From 1800 to 1300 cm^{-1}, the region where the dominant IR bands of oocyst functionalities occur (e.g., amides, carboxylates), the spectra exhibit a flat region without any major IR bands aside from the bending vibrations of CH_2 and CH_3 groups. The IR absorbances increase uniformly with decreasing pH, signaling increasing SDS surface excess with decreasing pH due to favorable electrostatic forces.[21]

The negatively charged sulfonate ($-OSO_3^-$) head of SDS is expected to form surface complexes on metal oxide surfaces. The ATR-FTIR technique is capable of determining whether an outer-sphere or inner-sphere complex forms. For example, the correlation between the symmetry of sulfate complexes and their IR spectra has been well-established.[28] Free aqueous SO_4^{2-} belongs to the point group T_d, which exhibits a triply degenerate asymmetric vibration (ν_3).[29] The symmetry of the sulfonate group in SDS is lowered to the C_{3v} point group, leading to a split of the ν_3 band into two: a doubly degenerate band at higher wavenumber and second non-degenerate band at lower wavenumber.[28,29] Since no direct bond results from outer-sphere (OS) complexation, the symmetry of the sulfonate remains similar to its aqueous form, and no new peak emerges in the spectra. If SDS were to form inner-sphere (IS) complexes at mineral surfaces, the symmetry of the sulfonate group would be further reduced to the C_{2v} point group, and the ν_3 band fully split to three bands between 1250 and 1050 cm^{-1}.[29,30] Therefore, the complexation mode (e.g., IS or OS) can be determined on the basis of the peak number and position of the ν_3 band. As shown in Figure S1 of the Supporting Information, asymmetric stretching of the sulfonate group results in a doublet (1238 and 1208 cm^{-1}), corresponding to the C_{3v} symmetry, indicating that SDS is adsorbed to hematite via outer-sphere complexation. This observation is also supported by the results of batch adsorption experiments that show that SDS does not promote release of OH^- or Fe(III) from hematite, which could be expected if ligand exchange at the hematite surface were operative.[21]

3.2. SDS−Oocyst Binary System. Adsorption of SDS to oocyst surfaces in suspension (no hematite) was measured as a function of pH in 10 mM NaCl background electrolyte. Adsorption decreases initially with increasing pH and then remains relatively constant (within error) at pH >6.0 (Figure 1). A similar trend was reported for NOM adsorption to *Bacillus subtilis*.[31] The decrease could be attributed to an increase in electrostatic repulsive force between the strongly acidic sulfonate group of SDS ($pK_a < 2.0$)[32] and the weakly acidic oocyst surface functional groups (amide, amino, phosphoryl, carboxyl) that are progressively deprotonated with increasing pH.[33] Despite like-charge repulsion, a significant amount of adsorption occurs at high pH, presumably as a result of hydrophobic or Na^+-bridging interactions. Batch results for pH-dependent SDS adsorption to hematite from the same background electrolyte solution[21] are included for comparison (Figure 1). In contrast, adsorption to hematite consistently decreases with increasing pH, and no substantial adsorption occurs at pH >9.0 (near the point of zero charge of α-Fe_2O_3), indicating that the adsorption is largely controlled by electrostatic attraction.

Adsorption of SDS on oocyst surfaces may affect the ζ-potential and hydrophobicity of oocyst cells. For example, a more negative ζ-potential and higher hydrophobicity were observed when 5 mg L^{-1} of NOM carbon was added to an oocyst suspension.[34] Such changes are expected to affect oocyst attachment and removal by substrate solid surfaces. Indeed, the authors reported that oocyst removal in columns packed with glass beads decreased from 51% in the absence of NOM to 14% in its presence. The decrease was attributed to an increase in electrostatic repulsion between oocysts and the negatively charged glass beads.

ATR-FTIR spectra of the viable *C. parvum* oocyst suspension on the ZnSe IRE in the absence and presence of 0.1 mM SDS are almost identical (Figure 2a,b), both containing IR bands corresponding to amides (1635, 1542, and 1337−1313 cm^{-1} for amide I, amide II, and amide III, respectively), carboxylate (COO^-

dx.doi.org/10.1021/la104907j |*Langmuir* 2011, 27, 5936–5943

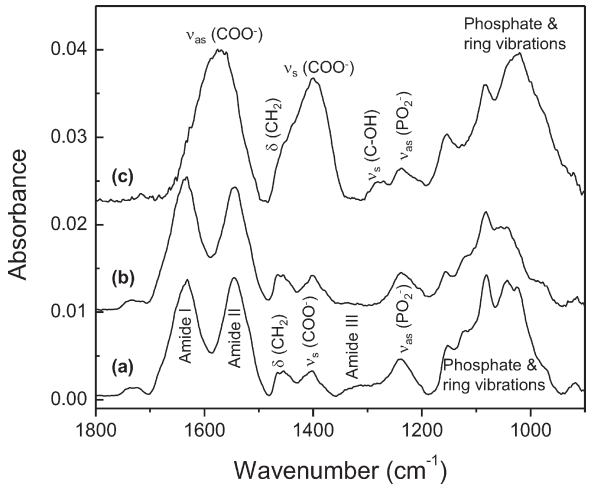

Figure 2. ATR-FTIR spectra of viable oocyst suspension in 10 mM NaCl solutions at pH 6.0 after 120 min reaction time on (a) ZnSe IRE in the absence of SDS (modified from Gao and Chorover[13]), (b) ZnSe IRE in the presence of 0.1 mM SDS (after subtraction the spectrum of 0.1 mM SDS), and (c) adsorbed to hematite surface in the absence of SDS (modified from Gao and Chorover[15]).

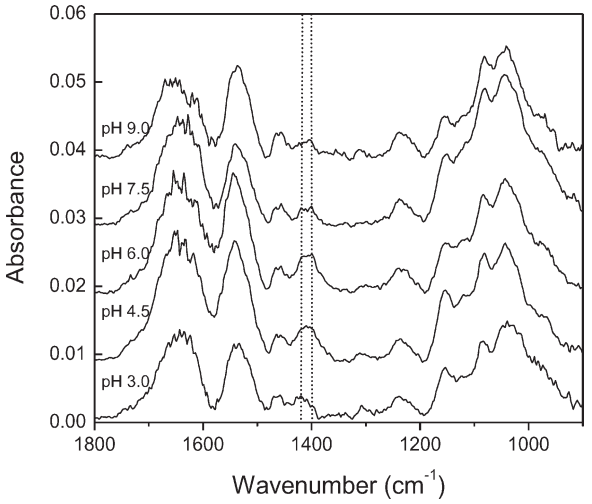

Figure 3. ATR-FTIR spectra of viable oocyst suspension on hematite surface in the presence of 0.01 mM SDS in 10 mM NaCl solution as a function of pH after 120 min reaction time. The gray bar indicates the peak position of $\nu_s(COO^-)$.

at 1400 cm^{-1}), phosphate (1237 cm^{-1}), and polysaccharide functional groups (C−O−C, C−C, 1150−950 cm^{-1}).[13] Öocyst adhesion to the ZnSe IRE is governed by a combination of DLVO (electrostatic and van der Waals) and electrosteric forces.[13] Thus, in contrast to column transport studies with NOM,[34,35] SDS−oocyst interaction does not detectably affect the ATR-FTIR signal of oocyst surface chemistry and adhesion at the negatively charged and moderately hydrophobic[13] ZnSe IRE surface.

3.3. Effect of SDS on Oocyst−Hematite Adhesion. As we reported previously, oocysts are adhered to hematite surfaces through inner- and outer-sphere complexation of carboxylate groups at Fe(III) metal centers.[15] This effect is illustrated in the present work by the fact that when hematite nanoparticles coat the ZnSe IRE, the oocyst spectrum (Figure 2c) is distinct from those for the uncoated IRE (Figure 2a,b). Specifically, when α-Fe_2O_3 surfaces are present, strong asymmetric and symmetric COO^- stretching bands emerge, signaling the formation of Fe−carboxylate complexes.[15] In addition, the complexation mode for hematite-adhered oocyst carboxylate groups can be assigned principally to bidentate binuclear complexation at pH 6.0,[15] based on the separation in wavenumber ($\Delta\nu$) of $\nu_{as}(COO^-)$ and $\nu_s(COO^-)$ stretching bands (e.g., $\Delta\nu > 200$ cm^{-1} for monodentate, 180−150 cm^{-1} for binuclear bidentate, and <100 cm^{-1} for mononuclear bidentate).[36,37]

Spectra of the oocyst−hematite interaction show major changes in the carboxylate stretching region resulting from the presence of 0.01 mM SDS (Figure 3). As shown in Figure 2c, in the absence of SDS, carboxylate stretching bands [both $\nu_{as}(COO^-)$ and $\nu_s(COO^-)$] are the dominant IR bands in the spectrum. Conversely, in the presence of SDS, the intensity of the asymmetric COO^- stretch after 120 min reaction time is dramatically reduced and masked by amide groups of proteins and the intensity of the symmetric stretching is significantly reduced as well (Figure 3). This diminished intensity of carboxylate stretching indicates that the presence of SDS effectively disrupts Fe−carboxylate complexation. In addition, similar to spectra obtained in the absence of SDS, the symmetric stretching vibration is represented by two bands (shown by dashed lines at 1418 and 1400 cm^{-1}) in the pH range of 3.0−7.5, indicating the presence of two inner-sphere complexes.[15,38,39] Notably, the band at 1418 cm^{-1} emerges while the one previously present at 1370 cm^{-1} in the absence of SDS[15] vanishes, suggesting that SDS alters the complexation mode between hematite and oocyst surface carboxylate groups (see below).

In addition, the intensity of the carboxylate stretching is strongest at the intermediate pH ∼6.0 (Figure 3), indicating that Fe−carboxylate complexation is more resistant to SDS disruption at this pH. This observation can be partially explained by the surface charge densities of oocysts and hematite, both of which are a function of pH. Lowering the charge on oocysts at the intermediate pH can reduce the repulsion between cells, enabling a higher surface excess. Furthermore, as shown in Figure 1, minimum SDS adsorption to oocyst cells occurs at pH ∼6.0, which may also contribute to stronger oocyst−hematite adhesion at this pH.

3.4. Kinetics of Oocyst−SDS−Hematite Ternary Interaction. To evaluate the time-dependency of the ternary interaction, we focused on the spectral region of $\nu_s(COO^-)$ (1500−1200 cm^{-1}), which is subject to minimal influence from the bending vibrations of H_2O (Figures 4a−e and 5). The intensity of the $\nu_s(COO^-)$ band for spectra collected on the ZnSe IRE in the presence of SDS reaches a plateau in ca. 15 min and remains constant thereafter (data not shown), which is consistent with adsorption being controlled by electrostatic interaction rather than specific surface complexation. As shown in Figure 5a, the absorbance of the symmetric COO^- stretch on hematite surface increases progressively with interaction time in the absence of SDS due to the progressive formation of Fe−carboxylate complexes. However, the opposite trend is observed in the presence of SDS. The symmetric stretching band decreases consistently with interaction time for all pH values, suggesting that Fe−carboxylate complexes are gradually diminished by the disruptive effects of the surfactant (Figure 5b).

With SDS present at pH 3.0, the symmetric COO^- stretching vibration is represented by two bands at 1418 and 1400 cm^{-1} (Figure 4a and Figure S2 in the Supporting Information), which indicates the presence of two inner-sphere complexes.[15] The

dx.doi.org/10.1021/la104907j |Langmuir 2011, 27, 5936–5943

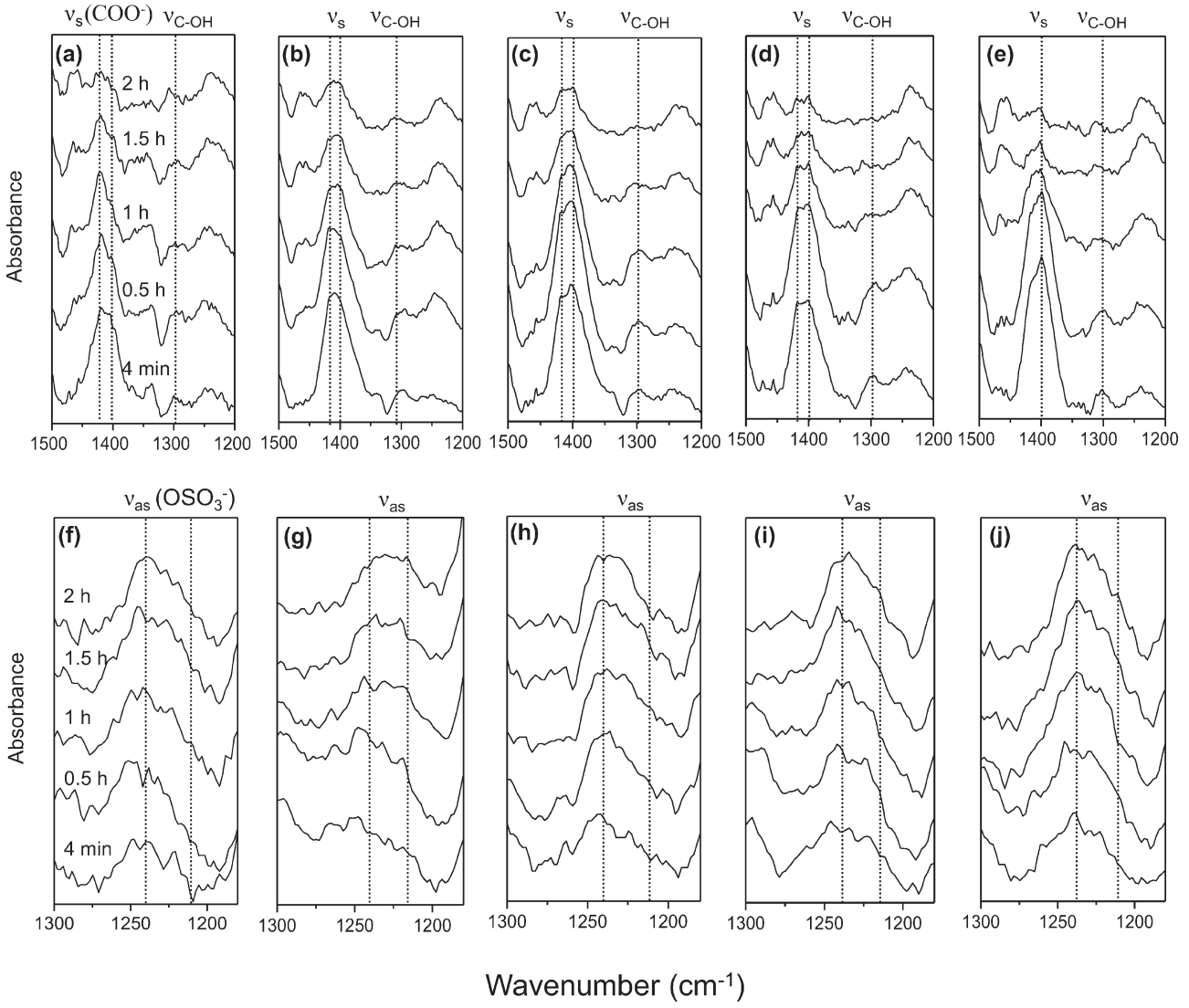

Figure 4. ATR-FTIR spectra of viable oocyst suspension reacted with hematite surface in the presence of 0.01 mM SDS in 10 mM NaCl solution as a function of reaction time (4 min to 2 h) in the region of $\nu_s(COO^-)$ (1500−1200 cm^{-1}) at (a) pH 3.0, (b) pH 4.5, (c) pH 6.0, (d) pH 7.5, and (e) pH 9.0 and $\nu_{as}(OSO_3^-)$ (1300−1180 cm^{-1}) at (f) pH 3.0, (g) pH 4.5, (h) pH 6.0, (i) pH 7.5, and (j) pH 9.0.

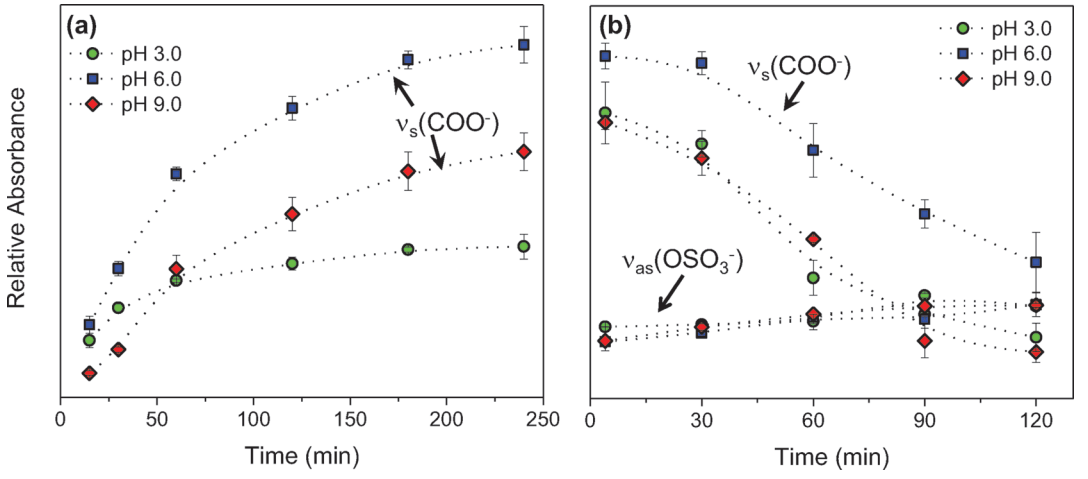

Figure 5. IR absorbance of $\nu_s(COO^-)$ and $\nu_{as}(OSO_3^-)$ of oocyst suspension reacted with hematite surface in 10 mM NaCl solution as a function of reaction time (a) in the absence of SDS and (b) in the presence of 0.01 mM SDS.

dx.doi.org/10.1021/la104907j |*Langmuir* 2011, 27, 5936–5943

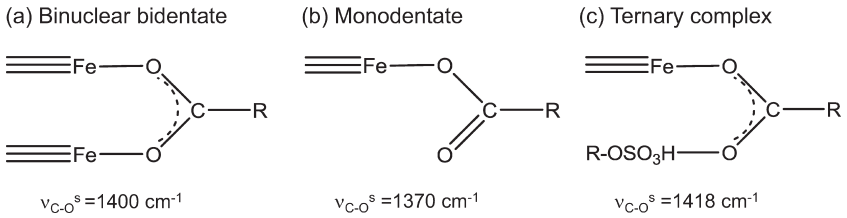

Figure 6. Schematic illustration of the surface complexation structures formed between carboxylate groups and hematite based on the $\Delta\nu$ of $\nu_{as}(COO^-)$ and $\nu_s(COO^-)$. The peak position associated with each complex is labeled in the figure.

position of the asymmetric COO^- stretch was determined to occur at 1577 cm^{-1} by spectral deconvolution (see Supporting Information Figure S2). Thus, based on the $\Delta\nu$ between ν_{as} and ν_s of COO^-, both peaks at 1418 ($\Delta\nu$ = 159 cm^{-1}) and 1400 cm^{-1} ($\Delta\nu$ = 177 cm^{-1}) could be potentially attributed to binuclear bidentate complexation.[36,37] Since the band at 1400 cm^{-1} decreases more rapidly than that at 1418 cm^{-1}, the complexation mode at 1418 cm^{-1} is evidently more stable at this pH. As discussed above, in the absence of SDS, we observed one binuclear bidentate complex (represented by the band at 1400 cm^{-1} with $\Delta\nu$ = 177 cm^{-1}) (Figure 6a) and one monodentate complex (represented by the band at 1370 cm^{-1} with $\Delta\nu$ = 207 cm^{-1}) (Figure 6b) with the monodentate complex dominating at pH 3.0.[15] The band at 1400 cm^{-1} persists in the presence of SDS, albeit at much lower intensity, whereas the band at 1370 cm^{-1} is eliminated, and a new band at 1418 cm^{-1} emerges. This might be interpreted as a change from monodentate to binuclear bidentate complex. However, this assignment is based on complex symmetry and does not require that both carboxylate oxygen atoms be bonded to Fe(III) centers. Indeed, if this were the case, it is not clear a priori why the band at 1418 cm^{-1} would be so strongly separated in frequency from that at 1400 cm^{-1}, which has precisely that assignment. Hence, we assert that this band at 1418 cm^{-1} could originate from carboxylate bonding to one Fe(III) and one hydroxyl proton, resulting in a symmetry that is similar—but not identical—to binuclear bidentate coordination with Fe(III) atoms. The participating hydroxyl groups in the ternary system may originate from either the hematite or SDS sulfonate groups. The fact that this band is absent in the binary oocyst−hematite system suggests that hematite surface hydroxyls do not form stable H-bonds with the oocyst carboxylate groups and participation of SDS sulfonate groups thus seems more likely. Hence, we postulate that the shift results from formation of an H-bond between the sulfonate groups of SDS and the carboxylate groups of the monodentate complex, forming a ternary, carboxylate−SDS−mineral complex (Figure 6c). This interpretation is consistent with the change of the dominant monodentate complex (i.e., band at 1370 cm^{-1}) in the absence of SDS at pH 3.0 to the dominant carboxylate−SDS−hematite ternary complex (i.e., band at 1418 cm^{-1}) in the ternary system after the introduction of SDS. Since natural soil and water systems contaminated with oocysts will rarely be acidic enough to reach pH 3.0, the adhesion mechanisms for such acidic conditions are expected to be likewise rarely observed in the natural environment.

Across the pH range, spectra all exhibit the same temporal trend of diminished symmetric COO^- stretching intensity with increasing reaction time (Figures 4b−e and 5b). Even in the pH range of 4.5−7.5, both bands at 1418 and 1400 cm^{-1} were still observed; however, the contribution from each complex is noticeably changed relative to the pH 3.0 case. With increasing pH, the binuclear bidentate complex represented by the band at 1400 cm^{-1} becomes stronger relative to the band at 1418 cm^{-1} (Figure 4a−e). There are two possible explanations for this observation. First, we found that high pH favors the binuclear bidentate complex in NaCl background electrolyte in the absence of SDS.[15] Second, progressive deprotonation of carboxyl groups and sulfonate with increasing pH hinders the formation of an H-bond between them and thereby reduces the contribution of the ternary complex. Indeed, when pH increases to 9.0, absorbance at 1400 cm^{-1} becomes the only dominant band.

In addition, the small band at ~1300 cm^{-1} present in all spectra irrespective of pH could be attributed to the stretching of ν_s(C−OH) (Figure 4a−e).[15,38,40] Similar to the $\nu_s(COO^-)$, the intensity of this band consistently decreases with reaction time, consistent with SDS diminishment of Fe−carboxylate complexation.

3.5. Molecular Mechanism of SDS Effect on Oocyst Adhesion. A recent column transport study indicated that the presence of SDS diminishes oocyst adhesion to a natural soil and increases cell transport.[25] The presence of SDS in the complex soil matrix may result in changes of surface charge, hydrophobicity, and surface structure of oocyst cells and substrate soil particles, all of which can be responsible for the increase in oocyst transport. Our ATR-FTIR spectroscopic data indicate that SDS diminishes the carboxylate−surface metal bonding at the microbe−mineral interface, which may also play a role in pathogen mobilization. The molecular mechanism responsible for the breaking of carboxylate−metal bonds is not yet clear, particularly since SDS evidently forms outer-sphere complexes with the hematite surface. Furthermore, although a significant amount of SDS is adsorbed by oocysts via electrostatic and hydrophobic interactions, the SDS−oocyst binary experiment indicates that the interaction between SDS and oocyst surface biomolecules has negligible impact on oocyst spectra when hematite is absent (Figure 2). Therefore, we speculate that the competitive adsorption between OSO_3^- groups of SDS and carboxylate groups at the oxide surface is the primary mechanism for the decrease of asymmetric and symmetric COO^- stretching in spectra of the ternary system. It is also likely that surfactant self-assembly at the hematite−water interface[21−23] contributes to the energetic favorability of carboxylate−Fe dissociation.

In order to examine the effect of the OSO_3^- group on Fe−carboxylate complexes, we focus on the spectral region of the asymmetric sulfonate stretching (1300−1180 cm^{-1}) as a function of time and pH (Figure 4f−j). As demonstrated in the SDS−hematite binary experiment, SDS forms outer-sphere complexes at the hematite surface, and the spectra exhibit a doublet $\nu_{as}(OSO_3^-)$ at 1238 and 1208 cm^{-1} (Supporting Information Figure S1). If the substitution of sulfonate for

dx.doi.org/10.1021/la104907j |*Langmuir* 2011, 27, 5936–5943

carboxylate occurs in the ternary system, the spectra should exhibit an increase of $\nu_{as}(OSO_3^-)$ with reaction time associated with the decrease of $\nu_s(COO^-)$ due to the formation of Fe−sulfonate complexation. As shown in Figure 5b, a slight increase of the $\nu_{as}(OSO_3^-)$ stretching bands with reaction time was observed, although the relative magnitude of this increase is small relative to the decrease in $\nu_s(COO^-)$ spectral intensity. One of the $\nu_{as}(OSO_3^-)$ bands (1238 cm^{-1}) overlaps with oocyst surface $\nu_{as}(PO_2^-)$ vibrations at ∼1237 cm^{-1}. While it is not possible to distinguish unambiguously the contribution of each band to the spectra, our prior work indicated that the $\nu_{as}(PO_2^-)$ stretching vibration does not change with time in the oocyst−hematite binary system with SDS absent.[15] It could however, decrease with time in an SDS-containing system, in a manner similar to what is observed for carboxylate. Thus, the time-dependent increase in absorbance intensity in this region of the spectrum (depicted in Figure 5b) can be considered as a conservative or low-end index of the progressive formation of hematite−sulfonate complexes. In addition, the other asymmetric OSO_3^- stretching band also increases with reaction time, indicated by the emergence of a shoulder peak at ∼1210 cm^{-1} in the spectra (Figure 4f−j). Although the displacement of inner-sphere by outer-sphere adsorbates seems energetically unfavorable, prior batch adsorption experiments indicate that sulfonate groups in surfactant molecules can exhibit higher affinity for mineral surfaces when compared to their carboxylate analogs, and the mechanisms responsible for the difference remain unknown.[41,42] It is possible that the OSO_3^- group may behave differently in the ternary system, more effectively forming inner-sphere Fe−sulfonate complexes to displace Fe−carboxylate bonds. As discussed above, if this occurs, the asymmetric stretching of OSO_3^- splits, to form an additional band between 1250 and 1050 cm^{-1}.[29,30] Unfortunately, due to the complexity of the ternary system spectra in this region, it is not possible for us to unambiguously determine the existence of the third asymmetric OSO_3^- band in the spectra.

4. CONCLUSIONS

A molecular-scale understanding of the effect of SDS on oocyst adhesion to the hematite surface in aqueous suspension was achieved using in situ ATR-FTIR spectroscopy. The extent of Fe−carboxylate surface complexation formed by reaction of oocyst surface biomolecules with hematite surface hydroxyls was significantly diminished in the presence of SDS. The primary mechanism for this effect is sulfonate group for carboxyl group substitution at the cell−mineral interface. Biosurfactants produced by soil microorganisms and plants are structurally comparable to SDS[43,44] and, therefore, may have similar effects on oocyst transport. Hence, our results suggest that low concentrations of these amphiphilic compounds may have profound impacts on oocyst adhesion and transport in the environment.

■ ASSOCIATED CONTENT

Supporting Information. Additional figures as discussed in the text. This material is available free of charge via the Internet at http://pubs.acs.org.

■ AUTHOR INFORMATION

Corresponding Author

*E-mail: chorover@cals.arizona.edu. Telephone: 520-626-5635. Fax: 520-621-1647.

■ ACKNOWLEDGMENT

Research funding was provided by the U.S. Department of Agriculture, National Research Initiative, Water and Watersheds Program (Grant #2006-35102-17192). We are grateful to Drs. Ronald Harvey and Chittaranjan Ray for stimulating discussions and collaborations regarding surfactant effects on *C. parvum* transport in the subsurface.

■ REFERENCES

(1) Redman, J. A.; Walker, S. L.; Elimelech, M. *Environ. Sci. Technol.* **2004**, *38*, 1777–1785.
(2) Ongerth, J. E.; Pecoraro, J. P. *J. Environ. Eng., ASCE* **1996**, *122*, 228–231.
(3) Tufenkji, N.; Dixon, D. R.; Considine, R.; Drummond, C. J. *Water Res.* **2006**, *40*, 3315–3331.
(4) Camesano, T. A.; Logan, B. E. *Environ. Sci. Technol.* **2000**, *34*, 3354–3362.
(5) Kuznar, Z. A.; Elimelech, M. *Environ. Sci. Technol.* **2006**, *40*, 1837–1842.
(6) Abudalo, R. A.; Bogatsu, Y. G.; Ryan, J. N.; Harvey, R. W.; Metge, D. W.; Elimelech, M. *Environ. Sci. Technol.* **2005**, *39*, 6412–6419.
(7) Mills, A. L.; Herman, J. S.; Hornberger, G. M.; Dejesus, T. H. *Appl. Environ. Microbiol.* **1994**, *60*, 3300–3306.
(8) Parikh, S. J.; Chorover, J. *Langmuir* **2006**, *22*, 8492–8500.
(9) Ojeda, J. J.; Romero-Gonzalez, M. E.; Purran, H. M.; Banwart, S. A. *Mineral. Mag.* **2008**, *72*, 101–106.
(10) Jucker, B. A.; Harms, H.; Hug, S. J.; Zehnder, A. J. B. *Colloids Surf., B.* **1997**, *9*, 331–343.
(11) Shroll, R. M.; Straatsma, T. P. *Biophys. J.* **2003**, *84*, 1765–1772.
(12) Casemore, D. P.; Wright, S. E.; Coop, R. L. In *Cryptosporidium and Cryptosporidiosis*; Fayer, R., Ed.; CRC Press: Boca Raton, FL, 1997, pp 65−92.
(13) Gao, X. D.; Chorover, J. *Colloids Surf., B* **2009**, *71*, 169–176.
(14) Jenkins, M. B.; Eaglesham, B. S.; Anthony, L. C.; Kachlany, S. C.; Bowman, D. D.; William, C. G. *Appl. Environ. Microbiol.* **2010**, *76*, 1926–1934.
(15) Gao, X. D.; Metge, D. W.; Ray, C.; Harvey, R. W.; Chorover, J. *Environ. Sci. Technol.* **2009**, *43*, 7423–7429.
(16) Wershaw, R. *Environ. Sci. Technol.* **1993**, *27*, 814–816.
(17) Sutton, R.; Sposito, G. *Environ. Sci. Technol.* **2005**, *39*, 9009–9015.
(18) Fuerstenau, D. W.; Colic, M. *Colloids Surf., A* **1999**, *146*, 33–47.
(19) Bai, B.; Hankins, N. P.; Hey, M. J.; Kingman, S. W. *Ind. Eng. Chem. Res.* **2004**, *43*, 5326–5338.
(20) Chatterjee, A.; Moulik, S. P.; Majhi, R.; Sanyal, S. K. *Biophys. Chem.* **2002**, *98*, 313–327.
(21) Gao, X. D.; Chorover, J. *J. Colloid Interface Sci.* **2010**, *348*, 167–176.
(22) Zhang, R.; Somasundaran, P. *Adv. Colloid Interface Sci.* **2006**, *123*, 213–229.
(23) Dobson, K. D.; Roddick-Lanzilotta, A. D.; McQuillan, A. J. *Vib. Spectrosc.* **2000**, *24*, 287–295.
(24) Johnson, W. P.; Martin, M. J.; Gross, M. J.; Logan, B. E. *Colloids Surf., A* **1996**, *107*, 263–271.
(25) Mohanram, A.; Ray, C.; Harvey, R. W.; Metge, D. W. *Abstracts with Programs, GSA 2010 Annual Meeting in Denver, CO*; Geological Society of America: Boulder, CO, 2010; Vol. 42, p 219.
(26) Geoghegan, M.; Andrews, J. S.; Biggs, C. A.; Eboigbodin, K. E.; Elloitt, D. R.; Rolfe, S.; Scholes, J.; Ojeda, J. J.; Romero-Gonzalez, M. E.; Edyvean, R. G. J.; *Faraday Discuss.* **2008**, *139*, 85–103.
(27) Schwertmann, U.; Cornell, R. M. *Iron Oxides in the Laboratory: Preparation and Characterization*; Wiley-VCH: Weinheim, Germany, 1991.
(28) Nakamoto, K. *Infrared and Raman Spectra of Inorganic and Coordination Compounds*; John Wiley and Sons: New York, 1986.
(29) Hug, S. J. *J. Colloid Interface Sci.* **1997**, *188*, 415–422.

(30) Peak, D.; Ford, R. G.; Sparks, D. L. *J. Colloid Interface Sci.* **1999**, *218*, 289–299.
(31) Borrok, D.; Aumend, K.; Fein, J. B. *Chem. Geol.* **2007**, *238*, 44–62.
(32) Lefebvre-Cases, E.; de La Fuente, B. T.; Cuq, J. L. *J. Food Sci.* **2001**, *66*, 555–560.
(33) Karaman, M. E.; Pashley, R. M.; Bustamante, H.; Shanker, S. R. *Colloids Surf., A* **1999**, *146*, 217–225.
(34) Dai, X.; Hozalski, R. M. *Water Res.* **2002**, *36*, 3523–3532.
(35) Abudalo, R. A.; Ryan, J. N.; Harvey, R. W.; Metge, D. W.; Landkamer, L. *Water Res.* **2010**, *44*, 1104–1113.
(36) Deacon, G. B.; Phillips, R. *Coord. Chem. Rev.* **1980**, *33*, 227–250.
(37) Chu, H. A.; Hillier, W.; Debus, R. J. *Biochemistry* **2004**, *43*, 3152–3166.
(38) Hwang, Y. S.; Liu, J.; Lenhart, J. J.; Hadad, C. M. *J. Colloid Interface Sci.* **2007**, *307*, 124–134.
(39) Hwang, Y. S.; Lenhart, J. J. *Langmuir* **2008**, *24*, 13934–13943.
(40) Dobson, K. D.; McQuillan, A. J. *Spectrochim. Acta, Part A.* **1999**, *55*, 1395–1405.
(41) Higgins, C. P.; Luthy, R. G. *Environ. Sci. Technol.* **2006**, *40*, 7251–7256.
(42) Ochoa-Herrera, V.; Sierra-Alvarez, R. *Chemosphere* **2008**, *72*, 1588–1593.
(43) Bodour, A. A.; Drees, K. P.; Maier, R. M. *Appl. Environ. Microbiol.* **2003**, *69*, 3280–3287.
(44) Read, D. B.; Gregory, P. J. *New Phytol.* **1997**, *137*, 623–628.